

Effect of strong electromagnetic fields on dilute-gas spectra: The three-level system*

Lewis Klein[†] and Michel Giraud

Laboratoire des Interactions Moléculaires, Université de Provence, Centre de St Jérôme, 13397 Marseille, France

Abraham Ben-Reuven[‡]

Department of Chemistry, Massachusetts Institute of Technology, Cambridge, Massachusetts 02139

(Received 14 January 1974)

The effect of a strong perturbing radiation field on spectral lines is studied using an extension of the Kubo-Zwanzig-Fano relaxation formalism. The problem of a dilute gas interacting with a strong perturbing field and a weak probe field is solved, assuming a separation of collisional and radiative processes, by introducing a classical-field renormalization technique. The solution is formulated entirely in terms of linear-response functions. This method is applied to the problem of the three-level absorber perturbed by a strong field and probed by a weak field. Multiphoton transitions, double resonance, and dynamic Stark effects can be treated as manifestations of this three-level problem.

I. INTRODUCTION

In a previous publication¹ (hereafter referred to as I), a method was presented for the calculation of nonlinear optical effects using the operator techniques of linear-response theory. In particular, the saturation of a two-level system was studied. It is our purpose here to extend this method to three-level systems interacting with a strong perturbing radiation field and a weak probe radiation field. The emphasis of this formalism is on the concept of single-molecule response (Green's) function, in distinction to density matrix,² light amplitude,³ and wave-function⁴ formulations of the prevailing theories. The present treatment departs from previous ones in obtaining a nonperturbative solution (cf. Lamb² and Javan³), expressed in a closed form (cf. Autler and Townes⁴), and including higher-harmonics terms (cf. Hansch and Toschek⁵). Therefore, all the above-cited theories can be obtained as special cases.

The spectroscopic technique of using a weak field to probe a system perturbed by a strong field is a powerful method of studying molecular relaxation parameters. This method is variously termed double resonance, laser amplification, or dynamic Stark effect, depending on the domain of interest. For example, when applied to plasmas (dynamic Stark effect) this method can be used to study the frequency and amplitude of the plasma oscillations, thus permitting an accurate diagnostic of the plasma. This effect has been analyzed in detail by Hicks, Hess, and Cooper⁶ using methods developed by Autler and Townes⁴ and Baranger and Mozer.⁷ When microwave transitions are studied by this method (double resonance) the shift and broadening of the absorption lines can be directly related to the atomic parameters of for-

bidden transitions. A theoretical treatment of this effect based on the Karplus-Schwinger solution⁸ for the density matrix under conditions of saturation has been given by Di Giacomo.⁹ For optically pumped transitions (laser amplification) the principal emphasis has been on atomic-state populations and the corresponding nonlinear effects, i.e., two-photon transitions. For this case, extensive theoretical treatments have been proposed with various domains of applicability. These have been summarized by Hansch and Toschek⁵ using a unified density-matrix treatment.

A major limitation in all the above theoretical analyses has been the *ad hoc* introduction of a non-Hermitian Hamiltonian to represent the effect of collisional broadening of the various transitions. This procedure implies certain assumptions necessary to untangle the radiation and collision processes which are made more explicit in this work.¹ In addition, it may lead to further unwarranted approximations such as neglecting all processes of cross relaxation (important in microwave spectra¹⁰ and in the case of partially overlapping lines¹¹). The principal advantages of the theory described here are first, the use of well-developed linear-response operator methods to express the nonlinear susceptibility of the gas in terms of physically accessible quantities at all intermediate stages of the calculation, i.e., background populations (unperturbed diagonal density-matrix elements) and linear-response relaxation matrices. Second, the diagrammatic method utilized here permits an explicit solution to all orders in the field strength.

Sec. II briefly reviews the nonlinear method presented in I and Sec. III discusses the various modifications in the analytical procedure which are necessary to discuss the two-field problem. A specific three-level case (without velocity ef-

facts such as Doppler broadening) is then chosen and the results presented in Sec. IV. Finally, the modifications necessary for the inclusion of the Doppler effect are qualitatively discussed.

II. NONLINEAR RESPONSE

A brief review of the Kubo-Zwanzig-Fano relaxation method¹²⁻¹⁴ extended to include nonlinear phenomena in dilute gases, will be presented. The method and notation follows I. Velocity effects are neglected in the following. Their inclusion will be discussed in Sec. VI.

A dilute gas sample of N molecules each with a dipole moment $\vec{\mu}$ in a classical time-dependent electric field $\vec{E}(k, t)$ will have an induced polarization,

$$\vec{P}(k, t) = (N/V) \text{Tr}[\vec{\mu} e^{-i\vec{k}\cdot\vec{R}} \delta\rho(t)], \quad (1)$$

where V is the volume, R the position of the molecule, and $\delta\rho(t)$ the time-dependent part of the density matrix of the sample. In the above we have assumed that in the absence of the external field the sample is in equilibrium. The density matrix is then separated into two parts,

$$\rho(t) = \rho_e + \delta\rho(t), \quad (2)$$

where ρ_e is the time-independent equilibrium part which satisfies the Liouville equation,

$$i \frac{\partial \rho_e}{\partial t} = L\rho_e = 0. \quad (3)$$

Here, L is the sample Liouvillian in the absence of the external field, defined for quantum systems as

$$LX = \hbar^{-1} [H, X], \quad (4)$$

X being any dynamical variable of the system with Hamiltonian H . L is thus a tetradic (Liouville-space) operator. The time-dependent part, $\delta\rho(t)$, satisfies the Liouville equation,

$$i \frac{\partial \delta\rho(t)}{\partial t} - L\delta\rho(t) = -\vec{M} \cdot \vec{E}(k, t) [\rho_e + \delta\rho(t)], \quad (5)$$

where

$$\vec{M}X = \hbar^{-1} \sum_{A=1}^N [\vec{\mu}_A e^{i\vec{k}\cdot\vec{R}_A}, X] \quad (6)$$

defines \vec{M} as a Liouville-space operator related to the dipole moment density. Note that the external electric field \vec{E} is treated classically and the interaction with the system has been written using the electric dipole approximation.

To simplify our treatment we shall introduce at this stage several assumptions:

(i) We shall concern ourselves only with the

“foreign-gas” broadening problem, i.e., we shall distinguish between the absorbing molecule and the perturbing molecules (which do not interact with the radiation). Removal of this restriction in dilute gases results in a small correction to the relaxation parameters.¹⁵

(ii) We shall consider here the resonance frequencies and damping coefficients as velocity independent. This assumption will be further discussed in Sec. VI.

(iii) We shall ignore, following Fano,¹⁴ statistical correlations between the absorber and the perturbers and write $\rho_e = \rho_s \rho_b$ where ρ_s pertains to the absorber (the “system”) and ρ_b to the perturbers (the “bath”). A detailed discussion of these phenomena (in the context of the linear-response theory) is given elsewhere.¹⁶

With the above assumptions we can drop the exponential k -dependent factors, and consider instead of the sum in (6) only a one-molecule term. We shall henceforth drop all reference to k .

We now Fourier-transform Eq. (5) and obtain

$$\delta\rho(\omega) = -G(\omega) \vec{M} \cdot \vec{E}(\omega) \rho_e + (2\pi)^{-1} \times \int_{-\infty}^{\infty} \vec{M} \cdot \vec{E}(\omega') \delta\rho(\omega - \omega') d\omega', \quad (7)$$

where

$$G(\omega) = (\omega + i\epsilon - L)^{-1} \quad (8)$$

is the Fourier transform of the Liouville-space propagator (or retarded tetradic Green’s function),

$$G(t) = -i\Theta(t)e^{-iLt}, \quad (9)$$

the $\Theta(t)$ being the Heaviside step function which vanishes for negative t . The solution of Eq. (7) by iteration leads to the following recurrence relation

$$\rho^{(j+1)}(\omega) = -(2\pi)^{-1} G(\omega) \int_{-\infty}^{\infty} \vec{M} \cdot \vec{E}(\omega') \times \rho^{(j)}(\omega - \omega') d\omega', \quad j=1, 2, \dots \quad (10)$$

The first iteration,

$$\rho^{(1)}(\omega) = -G(\omega) \vec{M} \cdot \vec{E}(\omega) \rho_e, \quad (11)$$

which is linear in the external field, is the Kubo solution for linear response and leads to the familiar expression for the i th Cartesian component of the polarization of the sample at the angular frequency ω ,

$$P_i(\omega) = -(N/V) \text{Tr}[\mu_i G(\omega) \vec{M} \cdot \vec{E}(\omega) \rho_e]. \quad (12)$$

The coefficient of the classical field, $E(\omega)$, in the above equation is defined as the linear-response susceptibility, $\chi^{(1)}(\omega)$, of the sample.

In I a method for calculating the nonlinear corrections to Eq. (12) was presented. The external

electric field is decomposed into a superposition of coherent monochromatic fields,

$$E(\omega) = \pi \sum_k [E_k^+ \delta(\omega - \omega_k) + E_k^- \delta(\omega + \omega_k)],$$

$$E_k^- = (E_k^+)^*, \quad (13)$$

which permits the nonlinear polarizability to be written in terms of a sum of δ functions with contributions from various combinations of harmonics of the fundamental frequencies, i.e.,

$$\vec{n} \cdot \vec{\omega} = \sum_k n_k \omega_k \quad (n_k = 0, \pm 1, \dots \text{ for each } k), \quad (14)$$

where

$$\vec{n} = (n_1, \dots, n_k, \dots) \quad (15a)$$

is a set of harmonics numbers and

$$\vec{\omega} = (\omega_1, \dots, \omega_k, \dots) \quad (15b)$$

is the set of fundamental frequencies of the field. The harmonics numbers defined above count numbers of photons added to or subtracted from the radiation field by absorption or emission (instead of absolute numbers of photons). Therefore, they can be considered as the classical Liouville-space analog of the occupation-number representation of quantum-field theory.

We may correspondingly introduce a harmonic-number representation (HNR), with basis vectors $|n\rangle$, in which the field E_k^\pm of Eq. (13) is redefined as an operator, \mathcal{E}_k^\pm , which raises or lowers the harmonics numbers by one unit:

$$\mathcal{E}_k^\pm |n_1, \dots, n_k, \dots\rangle = E_k^\pm |n_1, \dots, n_k \pm 1, \dots\rangle. \quad (16)$$

In the classical strong-field limit, \mathcal{E}_k^+ and \mathcal{E}_k^- commute. The interaction of the sample with the external field is expressed in terms of these field operators as

$$U = -\frac{1}{2} \sum_{\pm} \sum_k M_k \mathcal{E}_k^{\pm}. \quad (17)$$

To the equilibrium distribution ρ_e corresponds a HNR "vacuum" ($\vec{n}=0$), which will be denoted $|\vec{0}\rangle$. The Fourier component of the polarization at the harmonics combination of angular frequency $\vec{n} \cdot \vec{\omega}$ is given in HNR by

$$P_i(\vec{n} \cdot \vec{\omega}) = (N/V) \text{Tr}(\langle\langle \vec{n} | \mu_i \mathcal{G} U \rho_e | \vec{0} \rangle\rangle), \quad (18)$$

where the trace still refers only to the molecular-sample variables. In the above, \mathcal{G} is a renormalized Green's function obeying the Dyson equation,

$$\mathcal{G} = G + G U \mathcal{G}, \quad (19)$$

with the formal solution

$$\mathcal{G} = (G^{-1} - U)^{-1}. \quad (20)$$

The propagator G , previously introduced in Eq. (8) should be redefined as a diagonal operator in HNR,

$$G = (\Omega + i\epsilon - L)^{-1}, \quad (21)$$

where Ω is the diagonal operator whose eigenvalues are the harmonics frequencies,

$$\Omega |\vec{n}\rangle = \vec{n} \cdot \vec{\omega} |\vec{n}\rangle. \quad (22)$$

Thus, e.g.,

$$\langle\langle \vec{n}' | G | \vec{n} \rangle\rangle = \delta_{\vec{n}, \vec{n}'}, \quad G(\vec{n} \cdot \vec{\omega}). \quad (23)$$

Equation (18) is a basic result of I, representing the nonlinear polarization at the frequency $\omega = \vec{n} \cdot \vec{\omega}$.

As has been pointed out in I, the usual projection-operator techniques of Zwanzig and Fano can be applied to reduce the propagator G , which is defined on the molecular-sample variables, to an operator defined on the single-molecule space of the absorbing molecule, averaging out all the "bath" degrees of freedom. (The restriction to a single absorbing molecule is not essential, since, as already mentioned, the results can be readily extended to self-broadening, where the gas molecules are identical.) Using the techniques of Zwanzig and Fano, \mathcal{G} in Eq. (20) can be replaced by

$$D \mathcal{G} D = [\Omega - L_s - D U D - \Sigma_c(\Omega)]^{-1}. \quad (24)$$

Here, D is the projection operator onto the single-molecule subspace (in Liouville space), L_s is the (diagonal) matrix of molecular resonance frequencies, and $\Sigma_c(\Omega)$ is a tetradic proper self-energy (or "relaxation matrix") the Hermitian and anti-Hermitian parts of which have elements that, respectively, describe the various shift and relaxation rates.

An extremely useful approximation introduced in I is the assumption that the collisional and radiative processes may be disentangled. This amounts to writing,

$$D \mathcal{G} D \approx D G D + D G D U D \mathcal{G} D. \quad (25)$$

As a result of this, $\Sigma_c(\Omega)$ in Eq. (24) includes only contributions of pressure broadening. The terms neglected in Eq. (25) imply radiative corrections to the proper self-energy which are supposed to be small.

The operator D projects on the subspace of *all* single-molecule excitations, not only the dipole-allowed ones. In this subspace, U is invariant, but it may connect transitions with different multipole character. Consequently, $\Sigma_c(\Omega)$ should also be defined on the entire subspace, although (as a result of the thermal averaging) it is reducible to the various multipole subspaces.¹⁷

The Dyson equation, in the approximation of Eq. (25), can be written in a somewhat modified fashion required for the introduction of the renormalization techniques to be used later. Divide the HNR into two subspaces, the even and odd parts, in which $\sum_k n_k$ is even or odd, respectively. Introduce projection operators for these even and odd HNR subspaces, denoted \mathfrak{D}_e and \mathfrak{D}_o . Consider the projection of \mathfrak{g} onto either of these, e.g.,

$$\mathfrak{D}_o \mathfrak{g} \mathfrak{D}_o = \mathfrak{D}_o G \mathfrak{D}_o + \mathfrak{D}_o G U \mathfrak{g} \mathfrak{D}_o. \quad (26)$$

In the above, G , like \mathfrak{g} , is confined to one of the two subspaces, depending on its argument Ω . However, U has an odd "parity" in this representation. Therefore, in the expansion of \mathfrak{g} in a power series of U , only even powers of U will remain after the application of the projection operators. We can therefore rewrite Eq. (25) in the form

$$\mathfrak{D}_o D \mathfrak{g} \mathfrak{D}_o = \mathfrak{D}_o (DGD + DGDWD \mathfrak{g} \mathfrak{D}_o), \quad (27)$$

where the binary form

$$W = UDGDU, \quad (28)$$

replaces the original interaction U .

The above arguments are independent of any arguments concerning parity in the ordinary sense (i.e., in the molecular space). However, introduction of the molecular Green's functions can be further simplified if parity is a good quantum number of the gas sample. We may then divide the molecular projection-operator D into even and odd parts,

$$D = D_e + D_o.$$

Equation (27) now automatically separates the even and odd projections, $D_e \mathfrak{g} \mathfrak{D}_e$ and $D_o \mathfrak{g} \mathfrak{D}_o$, with the intermediate DGD in W of Eq. (28) being projected onto the opposite-parity subspace since U also has an odd parity in this representation. For the calculation of the polarization, we need the odd-parity projection,

$$D_o \mathfrak{g} \mathfrak{D}_o = [\Omega - L_s - W - \Sigma_c(\Omega)]^{-1}. \quad (24b)$$

Where D_e replaces D in Eq. (28) and Σ_c is now confined to the odd-parity subspaces. In this case, the introduction of a projection onto HNR "parity" subspace is, in fact, irrelevant. It is, however, necessary if parity is not a good quantum number of the molecular system in order to express the Dyson equation in terms of W .

The nonlinear polarization is now expressed completely in terms of quantities which can be calculated from linear-response theory. Consider, for example, the response to a single-field mode with frequency ω . The appropriate matrix ele-

ment of the polarization at the frequency ω is,

$$P_i(\omega) = -\frac{1}{2}(N/V) \sum_{\pm} \sum_j \text{Tr}(\langle\langle 1 | \mu_i D \mathfrak{g} D M_j \mathfrak{g}_j^{\pm} \rho_s | 0 \rangle\rangle), \quad (29)$$

where ρ_s is the one-molecule density matrix and Tr is a trace over one-molecule states.

Since we consider here a single coherent mode, the phase of the field is irrelevant and we can choose,

$$E_j^+ = E_j^- = E_j, \quad (30)$$

where E_j is the field amplitude. If we were to consider several modes with different phases, the difficulty can be taken care of with a unitary transformation using the harmonics numbers introduced in Eq. (15a). The details of this procedure are irrelevant here and will be omitted.

We may now define a nonlinear susceptibility,

$$\chi_{ij}(\omega) = -(N/V) \sum_{\pm} \text{Tr}(\langle\langle 1 | \mu_i D \mathfrak{g} D M_j \rho_s | \pm 1 \rangle\rangle), \quad (31)$$

relating P_i to E_j . The first term in $D \mathfrak{g} D$, which is DGD , gives the linear-response susceptibility [to which only the $|+1\rangle$ term in Eq. (31) contributes].

The harmonics-number matrix elements of the nonlinear terms can be evaluated by using a diagrammatic method described in I. This problem is distinct from the problem of evaluating the molecular linear-response Green's functions, DGD , which are defined on a different space and can be treated by well-developed methods such as the Liouville-space techniques.¹⁶ This enables one to completely separate the problems associated with harmonics of the radiation field from the molecular absorber problem and thus, avoid unnecessary assumptions regarding the molecular Green's functions.

III. TWO-FIELD PROBLEM: HARMONICS-NUMBER MATRIX ELEMENTS

We consider here the response of a dilute sample to a weak monochromatic probe field of magnitude E_1 and frequency ω_1 in the presence of a strong (saturating) field $E_2(\omega_2)$. We assume that the two modes are distinct (e.g., they have distinct frequencies). The expression for the susceptibility given in Eq. (31) is now generalized to describe the linear response to the probe field including the nonlinear effects due to the saturating field. Since we consider the response linear in E_1 , we can leave its phase arbitrary and choose the phase of E_2 to be zero so that, $E_2^+ = E_2^- = E_2$. In this case we now have,

$$P_i(\omega_1) = \sum_j \chi_{ij}(\omega_1) E_{1j} = -(N/V) \sum_{\pm} \sum_{i=1,2} \text{Tr}(\langle\langle 1_1, 0_2 | \mu_i D \mathfrak{g} D \vec{M} \cdot \vec{\mathfrak{g}}_i^{\pm} \rho_s | 0_1, 0_2 \rangle\rangle), \quad (32)$$

where $|n_1, n_2\rangle$ is a two-field HNR state. In the above, E_1 is treated in the linear approximation and hence, $D\mathcal{G}D\vec{M} \cdot \vec{\mathcal{E}}_1^\pm$ contains only one probe-field raising operator \mathcal{E}_1^+ and even numbers of saturating-field raising and lowering operators \mathcal{E}_2^\pm . For simplicity both fields will be taken to be co-linear and polarized in the \hat{z} direction.

To perform the harmonics-number matrix elements indicated in Eq. (32) the diagrammatic notation introduced in I will be used. Circles represent the HNR matrix elements of each $D\mathcal{G}D$ in the series expansion of $D\mathcal{G}D$ (to be denoted henceforth as G and \mathcal{G} , respectively, for brevity), solid lines represent an HNR matrix element of the interaction $U_2 = -\frac{1}{2}\vec{M} \cdot \vec{E}_2$, and a dashed line represents that of the interaction $U_1 = -\vec{M} \cdot \vec{E}_1$. The general diagram which results from taking the HNR matrix elements for the various contributions to the n th-order susceptibility at the probe-field frequency is shown in Fig. 1. The circles and lines in this diagram now represent operators which act in the single-molecule subspace only. To obtain the complete nonlinear susceptibility the sum of all paths leading from right to left in Fig. 1 should be performed for the diagram in each order and a sum over all orders is then to

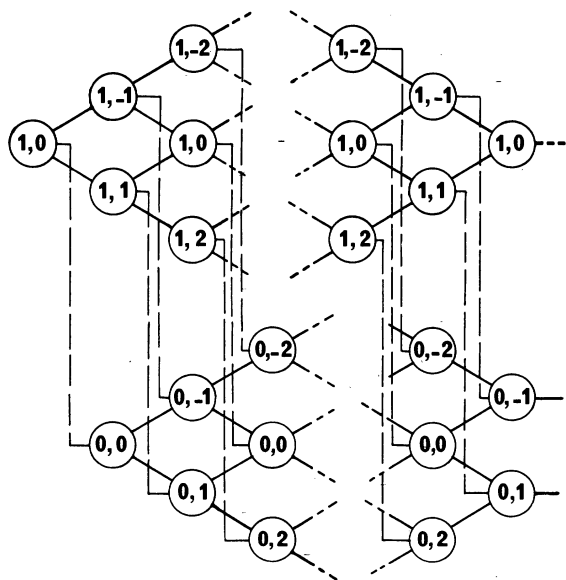


FIG. 1. Typical diagram for the linear response of a system to a monochromatic probe field, E_1 , in the presence of a strong saturation field, E_2 . Circles represent Green's functions $G(n_1, n_2)$. Connecting solid lines represent the interaction $U = -\frac{1}{2}\vec{M} \cdot \vec{E}_2$ and dashed lines represent $U_1 = -\vec{M} \cdot \vec{E}_1$. The diagram is composed of two networks, the upper network contains Green's functions of the form $G(1, n_2)$ and the lower network, Green's functions of the form $G(0, n_2)$. The two networks are connected only by the interaction U_1 .

be taken. These two summations can be performed by a method similar to the calculation of proper self-energy parts in quantum-field theory.

Note that the diagram in Fig. 1 is formed from two networks: one network, the upper one, contains only Green's functions of the form $G(1, n)$, where $n=0, \pm 1, \pm 2, \dots$. This network results from the action of \mathcal{E}_1^+ first in Eq. (32). The lower network contains only Green's functions of the form $G(0, \pm n)$ and is obtained when \mathcal{E}_2^\pm acts first. It is connected at one end to the upper network by a dotted line which represents the action of \mathcal{E}_1^+ . Since, as stated above, the susceptibility is the sum of all possible paths of all possible lengths in Fig. 1, we can reorder the summations so that we sum first with the position of the line representing \mathcal{E}_1^+ fixed. Consider the first case where \mathcal{E}_1^+ acts immediately to the right. This gives the sum of all paths of all possible lengths in the upper network only. This network will be denoted $\mathcal{G}(1, 0)$. It consists of $G(1, 0)$ plus all branches which begin with a $G(1, 0)$ and end with a $G(1, 0)$. This is illustrated diagrammatically in Fig. 2(a), where we used a double circle to represent $\mathcal{G}(1, 0)$ and the symbol \mathcal{W} to represent all branches connecting $G(1, 0)$ to $G(1, 0)$. The \mathcal{W} is called a "self-energy

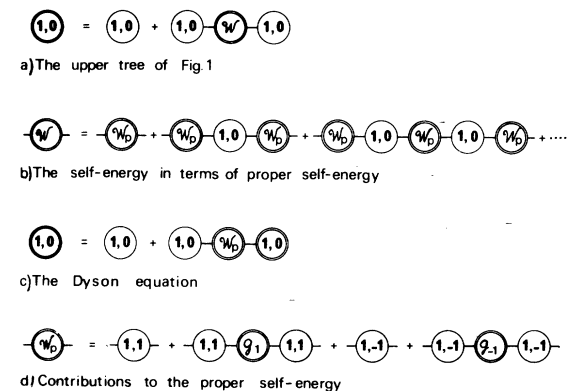


FIG. 2. (a) Sum of all diagrams of the type contained in the upper network of Fig. 1 which contribute to the linear response of a system to a monochromatic probe field E_1 in the presence of the saturating field E_2 . The double circle represents the sum of chains of linear-response Green's functions which are of length 1, 3, 5, etc. (b) Sum of chains of Green's functions described in (a) is expressed here in terms of proper self-energy insertions, \mathcal{W}_p . This is a sum of chains of linear-response Green's functions which cannot be broken into two chains by removing a Green's function, $G(1, 0)$. (c) Dyson equation which results from inserting the proper self-energy part into the diagram in (a). (d) Sum of the diagrams which are contained in the proper self-energy part of Fig. 2(c). Since \mathcal{W}_p contains no $G(1, 0)$ Green's-function links, $G(1, 1)$ is not connected to $G(1, -1)$ as can be seen from the upper network in Fig. 1.

insertion" in the language of quantum-field theory. As is usual \mathfrak{W} is now written in terms of a "proper self-energy insertion," \mathfrak{W}_p [i.e., a self-energy insertion which cannot be separated into two parts by removing one $G(1, 0)$ as is illustrated in Fig. 2(b)]. In terms of this proper self-energy insertion, Fig. 2(a) becomes the Dyson equation illustrated in Fig. 2(c) and can be written,

$$g(1, 0) = G(1, 0) + G(1, 0) \mathfrak{W}_p g(1, 0). \quad (33)$$

The calculation of \mathfrak{W}_p proceeds in exactly the same fashion. The contributions to \mathfrak{W}_p are illustrated in Fig. 2(d) where $g_{\pm 1}$ is the "polarization insertion" for \mathfrak{W}_p , containing all Green's-function branches which connect $W(1, \pm 1)$ to $W(1, \pm 1)$ without passing through $G(1, 0)$, where

$$W(1, \pm 1) = UG(1, \pm 1)U,$$

is the HNR matrix element of the binary interaction introduced in Eq. (28). In the above, and henceforth, we use U as a shorthand for U_2 . Since \mathfrak{W}_p contains no $G(1, 0)$ functions, no diagrams connecting $W(1, 1)$ to $W(1, -1)$ appear. Thus, \mathfrak{W}_p is the sum of the two terms which may be written as

$$\mathfrak{W}_p = \mathfrak{w}(1, 1) + \mathfrak{w}(1, -1), \quad (34)$$

where $\mathfrak{w}(1, 1)$ is defined by the first two terms in Fig. 2(d) and $\mathfrak{w}(1, -1)$ by the second two.

The contribution from the upper network in Fig. 1 can thus be written as

$$g(1, 0) = [G^{-1}(0, 1) - \mathfrak{w}(1, 1) - \mathfrak{w}(1, -1)]^{-1}. \quad (35)$$

It can be seen that the nonlinear contributions from the upper network simply renormalize the linear-response function. Thus, the functions $\mathfrak{w}(1, \pm 1)$ have Hermitian and anti-Hermitian parts which, in regions where the susceptibility is Lorentzian, play the role of radiative "shifts" and "widths." Since these functions also have resonances, there are regions of the spectrum where there will be "satellite" peaks occurring also. This interpretation is the classical-field counterpart of the "dressed-atom" concept introduced by Cohen-Tannoudji.¹⁸ The "dressed atom" is the

quantum-mechanical atom propagator renormalized by including intermediate multiphoton states. This physical interpretation will be discussed further below.

The function $\mathfrak{w}(1, \pm 1)$ in Eq. (34) can also be evaluated by using the same field theoretic techniques as for $g(1, 0)$. Thus, we can write a Dyson equation from Fig. 2(d) as follows:

$$\mathfrak{w}(1, \pm 1) = W(1, \pm 1) + W(1, \pm 1) g(1, \pm 2) \mathfrak{w}(1, \pm 1), \quad (36)$$

where $g(1, \pm 2)$ is the "proper polarization" part of $g_{\pm 1}$ in Fig. 2(d), and also satisfies a Dyson equation of the same form as Eq. (33). In fact, the renormalization can be carried out successively to account for all the possible branches in the upper network of Fig. 1. This procedure is equivalent to solving an alternating chain of Dyson equations for "proper self-energies" and "proper polarizations" of the form

$$g(1, \pm 2n) = G(1, \pm 2n) + G(1, \pm 2n) \times \mathfrak{w}[1, \pm(2n+1)] g(1, \pm 2n), \quad (37a)$$

$$\begin{aligned} \mathfrak{w}[1, \pm(2n-1)] &= W[1, \pm(2n-1)] \\ &+ W[1, \pm(2n-1)] g(1, \pm 2n) \\ &\times \mathfrak{w}[1, \pm(2n-1)] \quad (n=1, 2, \dots), \end{aligned} \quad (37b)$$

with solutions

$$g(1, \pm 2n) = \{G^{-1}(1, \pm 2n) - \mathfrak{w}[1, \pm(2n+1)]\}^{-1}, \quad (37c)$$

$$\mathfrak{w}[1, \pm(2n-1)] = \{W^{-1}[1, \pm(2n-1)] - g(1, \pm 2n)\}^{-1} \quad (n=1, 2, \dots). \quad (37d)$$

Substituting these solutions into Eq. (33) we obtain the solution for $g(1, 0)$, the upper network of Fig. 1, in the form of a continued fraction, or Padé approximant, in the linear-response Green's functions, as follows:

$$g(1, 0) = \frac{1}{G^{-1}(1, 0) - \frac{1}{W^{-1}(1, 1) - \frac{1}{G^{-1}(1, 2) - \frac{1}{\vdots}}}} - \frac{1}{W^{-1}(1, -1) - \frac{1}{G^{-1}(1, -2) - \frac{1}{\vdots}}} \quad (38)$$

Recall that the summations have been reordered so as to be performed with the position of U_1 fixed relative to a particular type of Green's function. The first case, calculated above, was the case in

which U_1 acted first and involved $g(1, 0)$ only, i.e., the upper network in Fig. 1. The next case is that in which U_1 acts to connect a Green's function in the lower network to $g(1, 0)$ either directly, if U_1

acts after $g(0,0)$, or through a chain of upper-network Green's functions starting with $G(1, \pm n)$ if U_1 acts after $G(0, \pm n)$.

We can classify the various contributions to the polarization according to the arguments of the specific pair of lower- and upper-network Green's functions connected by U_1 . The particular position of this pair in a branch running from right to left in Fig. 1 can be made irrelevant by using renormalized Green's functions. For this purpose we write Dyson equations for the lower network analogous to Eqs. (33), (37a), and (37b),

$$\mathfrak{w}(0,0) = W(0,0) + W(0,0)[g(0,1) + g(0,-1)]\mathfrak{w}(0,0), \quad (39a)$$

where the "proper polarization" $g(0,1) + g(0,-1)$ cannot be divided into two parts by removing a $W(0,0)$ interaction. Similarly,

$$\mathfrak{w}(0, \pm 2n) = W(0, \pm 2n) + W(0, \pm 2n) \times g[0, \pm(2n+1)]\mathfrak{w}(0, \pm 2n), \quad (39b)$$

$$g[0, \pm(2n-1)] = G[0, \pm(2n-1)] + G[0, \pm(2n-1)] \times \mathfrak{w}(0, \pm 2n)g[0, \pm(2n-1)] \quad (n=1, 2, \dots). \quad (39c)$$

The formal solutions corresponding to the above

$$\begin{aligned} \chi(\omega_1) = & -(N/V) \text{Tr} \{ \mu g(1,0) [1 + \mathfrak{w}(1,1)(1 + g(1,2)\{1 + \dots\}\mathfrak{w}(0,2))g(0,1) \\ & + \mathfrak{w}(1,-1)(1 + g(1,-2)\{1 + \dots\}\mathfrak{w}(0,-2))g(0,-1)] \\ & \times [1 + \mathfrak{w}(0,0)(g(0,+1) + g(0,-1))] M \rho_s \}. \end{aligned} \quad (42)$$

The single term $g(1,0)$ is the contribution from the upper network in Fig. 1; the rest of the terms are the interference terms coming from the lower network. Within the approximations stated in Sec. II, this result is perfectly general and expresses the effect of the frequency mixing which results from the strong saturating field. Since Eq. (42) contains Green's functions and interactions which operate only in the single-molecule Liouville subspace, it is now possible to perform the indicated trace operation. The rearrangement of diagrams which was performed above considerably simplifies this calculation, as will be seen.

The physical interpretation of the result can be easily seen since it has been expressed in terms of linear-response Green's functions. Thus, the upper network, Eq. (38) can be interpreted as the linear response at the weak-field frequency modified by the system response to one weak-field photon and successively one, two, etc., strong-field photons. It is for this reason that we referred

equations are the continued fractions analogous to Eqs. (37c), (37d), and (38),

$$\mathfrak{w}(0,0) = [W^{-1}(0,0) - g(0,1) - g(0,-1)]^{-1}, \quad (40a)$$

$$\mathfrak{w}(0, \pm 2n) = \{W^{-1}(0, \pm 2n) - g[0, \pm(2n+1)]\}^{-1} \quad (n=1, 2, \dots), \quad (40b)$$

$$g[0, \pm(2n-1)] = \{G^{-1}[0, \pm(2n-1)] - \mathfrak{w}(0, \pm 2n)\}^{-1}. \quad (40c)$$

The sum of all the direct connections of the lower network to the upper network (i.e., those involving $G(0,0)$ and $G(1,0)$ contributes the following term to the polarization,

$$g(1,0)\mathfrak{w}(0,0)[g(0,1) + g(0,-1)]. \quad (41a)$$

The connection via $G(0, \pm 1)$ and $G(1, \pm 1)$ contributes,

$$g(1,0)\mathfrak{w}(1, \pm 1)g(0, \pm 1)\{1 + \mathfrak{w}(0,0)[g(0,1) + g(0,-1)]\}. \quad (41b)$$

Succeeding contributions result from renormalized functions intervening between $\mathfrak{w}(1, \pm 1)$ and $g(0, \pm 1)$ in the chain of (41b). Thus, the complete susceptibility which is the sum of all these contributions plus $g(1,0)$ of Eq. (38), can be written as the infinite product,

to this result as the classical counterpart of the Cohen-Tannoudji, "dressed atom." That is, the linear response is successively renormalized by multiphoton intermediate states. The interference terms in Eq. (42) can be interpreted as the effect of saturation since only strong-field photons are included in the lower tree. This can best be seen by referring to the diagrams in I, p. 761, which contribute to two-level saturation. These terms express the effect of the "spectator" photons mentioned by Cohen-Tannoudji in his dressed-atom theory. As will be seen in Sec. IV, these terms can be neglected for certain level configurations in the atomic system. Finally, Eq. (38) bears a formal resemblance to the Autler-Townes⁴ solution for the ac Stark effect.

IV. THREE-LEVEL ATOMIC SYSTEM

In order to calculate the single-molecule Liouville-space matrix elements in Eq. (42), we must specify an atomic-level configuration. For the

purpose of comparing our results with previous work, a three-level atomic system will be considered. We restrict our attention here to the three atomic levels which are described by parity eigenstates arranged as in Fig. 3. The transitions $a-b$ and $b-c$ (of energy, respectively, ω_{ab} and ω_{bc}) are assumed to be dipole allowed and hence, transition $a-c$ will be dipole forbidden. The extension of this model to the case of folded arrays (b above a or below c) is straightforward and is treated in Ref. 5, among others.

The problem of space degeneracy has been discussed in I, Sec. VII. In the following we shall proceed as if the degeneracy is absent, for simplicity. However, if we were to consider the level degeneracy it would only cause the Green's-function tetrads to become matrices of larger dimensionality. To see this, suppose we associate with each transition $a-b$ in the nondegenerate case, the Liouville vector $|ab^+\rangle$ (using the notation suggested by Baranger.¹¹ In the degenerate case, we have to associate with the pair of energy levels a, b the whole degenerate manifold $|am_a(bm_b)^+\rangle$, with $m_a = -j_a, -j_a + 1, \dots, j_a$ (where j_a, m_a are the total angular momentum quantum numbers in the molecular center of mass coordinates), etc. Multipole subspaces, $|ab^+; jm\rangle$ can be formed¹⁷ with j running from $|j_a - j_b|$ to $j_a + j_b$. In this multipole representation, the G 's are invariant (diagonal in j and m , and independent of m). However, each time the Liouville-space operator M is applied it lowers or raises j by one unit. It is possible, in principle, to extend the diagrammatic analysis to take this into account. The nondegenerate scheme followed here is equivalent to neglecting all multipole subspaces other than the dipole ($j=1$) for odd-parity G 's and the monopole ($j=0$) for even parity G 's (those occurring in W).

In order to evaluate the single-molecule Liouville-subspace matrix elements of the renormalized Green's functions, we note that since the interaction, $U = -\frac{1}{2}\vec{M} \cdot \vec{E}_2$, is a parity changing operator and ρ_s has an even parity (in its diagonal representation), the Green's functions of Eq. (37a) operate on odd-parity Liouville-space vectors.

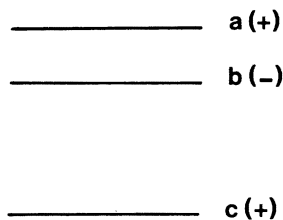


FIG. 3. Configuration and parity of the three-level system discussed here.

The Green's functions in the W of Eq. (37b) operate on even-parity vectors.

We now decompose the 9×9 single-molecule Liouville subspace of the three-level system into a 4×4 odd-parity subspace with basis vectors $|ab^+\rangle$, $|ba^+\rangle$, $|bc^+\rangle$, and $|cb^+\rangle$ and a 5×5 even-parity subspace with basis vectors $|aa^+\rangle$, $|bb^+\rangle$, $|cc^+\rangle$, $|ac^+\rangle$, and $|ca^+\rangle$.

The Green's-function matrix for the odd-parity subspace is

$$G(n_1, n_2) = [(n_1\omega_1 + n_2\omega_2)I - L_{s1} - \Delta_1 + i\Gamma_1]^{-1}, \quad (43)$$

$$n_1 = 1, \quad n_2 = \pm \text{even},$$

$$n_1 = 0, \quad n_2 = \pm \text{odd},$$

where I is the unit matrix, and L_{s1} is the matrix of resonance frequencies,

$$L_{s1} = \begin{bmatrix} \omega_{ab} & 0 & 0 & 0 \\ 0 & -\omega_{ab} & 0 & 0 \\ 0 & & \omega_{bc} & 0 \\ 0 & 0 & 0 & -\omega_{bc} \end{bmatrix} \quad (44)$$

and

$$\Gamma_1 = \begin{bmatrix} \gamma_{ab} & -\xi_{ab;ba} & \xi_{ab;bc} & \xi_{ab;cb} \\ -\xi_{ab;ba}^* & \gamma_{ab} & \xi_{ab;cb}^* & \xi_{ab;bc}^* \\ \xi_{ab;bc} & \xi_{ab;cb} & \gamma_{bc} & -\xi_{bc;cb} \\ \xi_{ab;cb}^* & \xi_{ab;bc}^* & -\xi_{bc;cb}^* & \gamma_{bc} \end{bmatrix} \quad (45)$$

is the matrix of relaxation and cross-relaxation rates. Δ_1 is the matrix of pressure shifts with a structure similar to Γ_1 .

We emphasize here, that generally, neither the binary-collision assumption, nor the impact approximation have to be implied in the above. Thus, e.g., the Γ matrix is not necessarily proportional to the perturber gas density nor frequency independent. Therefore, the present theory can be applied, for example, to nonlinear effects involving atoms in partially ionized plasmas where the binary-collision approximation is not necessary for the electrons and the impact approximation is invalid for the ions. For most gases at low pressures, the binary-collision impact theory is valid and Δ_1 and Γ_1 can be calculated in terms of binary-collision matrix elements.^{14,16} In the impact approximation,¹¹ Δ_1 and Γ_1 are independent of ω .

If the lines are sufficiently sharp so that $|\omega_{ab} \pm \omega_{bc}| \gg \gamma_{ab} + \gamma_{bc}$ then we can neglect the off-diagonal elements in Γ_1 and Δ_1 and obtain for the odd-parity subspace,

$$\begin{aligned} \langle\langle if^+ | G(n_1, n_2) | if^+ \rangle\rangle &= (n_1 \omega_1 + n_2 \omega_2 \\ &\quad - \omega_{if} - \delta_{if} + i \gamma_{if})^{-1} \\ &\equiv G_{if}(n_1, n_2), \end{aligned} \quad (46)$$

$$n_1 = 1, \quad n_2 = \pm \text{even},$$

$$n_1 = 0, \quad n_2 = \pm \text{odd},$$

where $|if^+\rangle$ is $|ab^+\rangle$, $|ba^+\rangle$, $|bc^+\rangle$, or $|cb^+\rangle$.

For particular values of the level spacing, linewidth, and perturbing field frequency ω_2 not all four of the odd-parity Green's functions above will be near resonance. Thus a major approximation to be applied later involves the neglect of off-resonance terms. Which of the functions are to be retained will be indicated later when a particular example is considered.

The Green's-function matrix for the even-parity subspace is

$$G(n_1, n_2) = [(n_1 \omega_1 + n_2 (\omega_2) I - L_{s0} - \Delta_0 + i \Gamma_0)]^{-1}, \quad (47)$$

$$n_1 = 1, \quad n_2 = \pm \text{odd},$$

$$n_1 = 0, \quad n_2 = \pm \text{even},$$

where

$$L_{s0} + \Delta_0 = \begin{bmatrix} \omega_{ac} + \delta_{ac} & 0 & \cdots & \cdots & \cdots \\ 0 & -\omega_{ac} + \delta_{ac} & \cdots & \cdots & \cdots \\ \cdots & \cdots & 0 & 0 & 0 \\ \cdots & \cdots & 0 & 0 & 0 \\ \cdots & \cdots & 0 & 0 & 0 \end{bmatrix}, \quad (48)$$

and

$$\Gamma_0 = \begin{bmatrix} \gamma_{ac} & \cdots & \cdots & \cdots & \cdots \\ \cdots & \gamma_{ac} & \cdots & \cdots & \cdots \\ \cdots & \cdots & \gamma_a & -\sigma_{ab} & -\sigma_{ac} \\ \cdots & \cdots & -\sigma_{ab}^* & \gamma_b & -\sigma_{bc} \\ \cdots & \cdots & -\sigma_{ac}^* & -\sigma_{bc}^* & \gamma_c \end{bmatrix}, \quad (49)$$

where γ_{ac} is the linewidth of the forbidden transition $a-c$, γ_a is the relaxation rate of level a , etc., and the σ 's are corresponding cross-relaxation rates. Unlike the simplification used in Eq. (45) we cannot here neglect *all* off-diagonal matrix elements. In the case of sharp nonoverlapping resonances we still must consider the off-diagonal elements explicitly written in Eq. (49). In the case, $n_1 = n_2 = 0$, only the three zero-resonance terms $|aa^+\rangle$, $|bb^+\rangle$, and $|cc^+\rangle$ contribute,

$$\langle\langle ii^+ | G(0, 0) | ff^+ \rangle\rangle = i (\Gamma_0^{-1})_{if} = G_{if}(0, 0), \quad (50)$$

where

$$\Gamma_0 = \begin{pmatrix} \gamma_a & -\sigma_{ab} & -\sigma_{ac} \\ -\sigma_{ab}^* & \gamma_b & -\sigma_{bc} \\ -\sigma_{ac}^* & -\sigma_{bc}^* & \gamma_c \end{pmatrix}.$$

Similarly,

$$\begin{aligned} \langle\langle if^+ | G(1, n_2) | if^+ \rangle\rangle &= (\omega_1 + n_2 \omega_2 - \omega_{if} - \delta_{if} + \gamma_{if})^{-1} \\ &= G_{if}(1, n_2) \quad (n_1 = 1, \quad n_2 = \pm \text{odd}), \end{aligned} \quad (51)$$

where, here, $|if^+\rangle$ is either $|ac^+\rangle$ or $|ca^+\rangle$.

We have given now all the matrix elements which occur in the various Dyson equations.

It has been remarked previously that ω_1 and ω_2 are to be considered as distinct frequencies. In addition, it will now be assumed that ω_{ab} and ω_{bc} are distinct transitions and that $\omega_{ab} < \omega_{bc}$. The contrary case could equally well be treated by the same transformation as that used to treat folded arrays. If now, ω_1 is used to probe a region covering ω_{bc} and ω_{ac} and we assume that $\omega_2 < \omega_{bc}$ (i.e., ω_2 is used either to saturate the $a-b$ transition or is a strong off resonant field), the number of near-resonance Green's functions that must be included is considerably reduced. For these conditions, in fact, we need consider only the following, at odd-parity stages,

$$G_{bc}(1, n_2) \quad (n_2 = 0, \pm 2, \pm 4, \dots, \text{even}), \quad (52a)$$

$$G_{ab}(0, 1), \quad (52b)$$

$$G_{ba}(0, -1), \quad (52c)$$

and at even-parity stages,

$$G_{if,ff}(0, 0) \quad (i, f = a, b, c), \quad (52d)$$

$$G_{ac}(1, n_2) \quad (n_2 = \pm 1, \pm 3, \dots, \text{odd}). \quad (52e)$$

Equation (52a) implies that there will be spectral resonances near $\omega_1 = \omega_{bc}$ (the resonance line) and $\omega_1 = \omega_{bc} \pm n_2 \omega_2$, where n_2 is an even integer, and Eq. (52e) implies resonances near $\omega_1 = \omega_{ac} \pm n_2 \omega_2$, where n_2 is an odd integer. It can thus be seen that a simple parity argument is the reason for which even numbers of photons of the strong field contribute "satellites" symmetrically placed about the resonance line, while odd numbers of photons yield satellites symmetrically placed about the forbidden-line position. In addition, as shall be seen later, complicated effects such as dynamic Stark widths and shifts are also contained in combinations of these functions. The Green's functions in Eqs. (52b)–(52d) are those which contribute to the saturation of the (a, b) pair of levels, as can be seen by comparison with the two-level theory in I.

The fact that Eqs. (52a)–(52e) list the only Green's-function matrix elements needed, con-

siderably simplifies the calculation of the susceptibility. To see this, consider the contribution from the first term in Eq. (42),

$$\text{Tr}[\mu \mathcal{G}(1, 0) M \rho_s] = \langle \mu | \mathcal{G}(1, 0) | M \rho_s \rangle,$$

where μ is represented in Liouville-space by the bra vector,

$$\langle \mu | = \mu_{ab} \langle ab^+ | + \mu_{ba} \langle ba^+ | + \mu_{cb} \langle bc^+ | + \mu_{bc} \langle cb^+ | \quad (53)$$

and $M \rho_s$ by the ket vector,

$$| M \rho_s \rangle = (\mu_{ab} | ab^+ \rangle - \mu_{ba} | ba^+ \rangle)(\rho_b - \rho_a) + (\mu_{bc} | bc^+ \rangle - \mu_{cb} | cb^+ \rangle)(\rho_c - \rho_b) \quad (54)$$

Since $\mathcal{G}(1, 0)$ satisfies the Dyson equation (33), a $G(1, 0)$ Green's function acts both to the right and to the left. From Eq. (52a), we see that $\mathcal{G}(1, 0)$ therefore selects the $| bc^+ \rangle$ state from $| M \rho_s \rangle$ and is diagonal in $| bc^+ \rangle$, thus

$$\langle \mu | \mathcal{G}(1, 0) | M \rho_s \rangle = |\mu_{bc}|^2 \langle bc^+ | \mathcal{G}(1, 0) | bc^+ \rangle (\rho_c - \rho_b), \quad (55)$$

where

$$\langle bc^+ | \mathcal{G}(1, 0) | bc^+ \rangle = [G_{bc}^{-1}(1, 0) - \langle bc^+ | \mathcal{W}(1, 1) + \mathcal{W}(1, -1) | bc^+ \rangle]^{-1}.$$

Note that the contribution in Eq. (55) is proportional to the unperturbed population difference in the lower two atomic states, $\rho_c - \rho_b$. Since in Eq. (42) all other terms have $G(0, \pm 1)$ acting on $| M \rho_s \rangle$, the states $| ab^+ \rangle$ or $| ba^+ \rangle$ will be selected, and from Eq. (54) it can be seen that these terms will all be proportional to $\rho_b - \rho_a$, the unperturbed population difference in the upper two atomic states. Thus, the complete susceptibility can be written,

$$\chi = -\hbar^{-1} (N/V) [R_{cb}(\rho_c - \rho_b) + R_{ba}(\rho_b - \rho_a)], \quad (56)$$

$$R_{cb} = \frac{|\mu_{bc}|^2}{G_{bc}^{-1}(1, 0) - \frac{\beta^2}{G_{ac}^{-1}(1, 1) - \frac{\beta^2}{G_{bc}^{-1}(1, 2) - \frac{\beta^2}{\ddots}}}} - \frac{\beta^2}{G_{ac}^{-1}(1, -1) - \frac{\beta^2}{G_{bc}^{-1}(1, -2) - \frac{\beta^2}{\ddots}}} \quad (59)$$

This contribution to the susceptibility, R_{cb} , comes only from the upper network in Fig. 1.

The rest of the terms in Eq. (42) which include interference from the lower network in Fig. 1 are proportional to $\rho_b - \rho_a$, the unperturbed population difference of the upper two states. They, thus,

where the matrix element in Eq. (55) is the only contribution to R_{cb} . The function $\mathcal{W}(1, \pm 1)$ in Eq. (55) is the renormalized interaction defined in Eq. (36). A calculation of its matrix elements involves a knowledge of the effect of M , which transforms between even- and odd-parity subspace vectors as follows:

$$\begin{aligned} \hbar M | aa^+ \rangle &= \mu_{ba} | ba^+ \rangle - \mu_{ab} | ab^+ \rangle, \\ \hbar M | cc^+ \rangle &= \mu_{bc} | bc^+ \rangle - \mu_{cb} | cb^+ \rangle, \\ M | bb^+ \rangle &= -M | aa^+ \rangle - M | cc^+ \rangle, \\ \hbar M | ac^+ \rangle &= \mu_{ba} | bc^+ \rangle - \mu_{cb} | ab^+ \rangle, \\ \hbar M | ca^+ \rangle &= \mu_{bc} | ba^+ \rangle - \mu_{ab} | cb^+ \rangle, \\ \hbar M | ab^+ \rangle &= \mu_{ba} | bb^+ \rangle - \mu_{ba} | aa^+ \rangle - \mu_{bc} | ac^+ \rangle, \\ \hbar M | ba^+ \rangle &= \mu_{cb} | ca^+ \rangle - \mu_{ab} | bb^+ \rangle + \mu_{ab} | aa^+ \rangle, \\ \hbar M | bc^+ \rangle &= \mu_{ab} | ac^+ \rangle - \mu_{cb} | bb^+ \rangle + \mu_{cb} | cc^+ \rangle, \\ \hbar M | cb^+ \rangle &= \mu_{bc} | bb^+ \rangle - \mu_{bc} | cc^+ \rangle - \mu_{ba} | ca^+ \rangle. \end{aligned} \quad (57)$$

Using these relations, the resonant conditions of Eq. (52d), and the Dyson Eq. (36) we obtain,

$$\langle bc^+ | \mathcal{W}(1, \pm 1) | bc^+ \rangle = [\beta^{-2} G_{ac}^{-1}(1, \pm 1) - \langle bc^+ | \mathcal{G}(1, \pm 2) | bc^+ \rangle]^{-1}, \quad (58)$$

where

$$\beta^2 = \left| \frac{\mu_{ab} E_2}{2\hbar} \right|^2$$

is the strong-field interaction parameter. In the above equation we have retained only the $| bc^+ \rangle$ matrix element of $\mathcal{G}(1, \pm 2)$, anticipating the near-resonance condition, Eq. (52a), and the Dyson equation for $\mathcal{G}(1, \pm 2)$.

Continuing this procedure for all terms in the series of Dyson equations we obtain terms which alternately select the vectors $| ac^+ \rangle$ and $| bc^+ \rangle$. The final result corresponding to Eq. (38) is

represent the interference effect of saturation of the (a, b) transition on the spectra probed by ω_1 in the vicinity of the (a, c) and (b, c) transitions.

Because of the near-resonance conditions implied in Eqs. (52a)–(52e), only the following interference terms need be considered,

$$\langle\langle \mu | \varrho(1, 0) [\mathfrak{W}(1, 1) \varrho(0, 1) + \mathfrak{W}(1, -1) \varrho(0, -1)] \{ \mathfrak{W}(0, 0) [\varrho(0, 1) + \varrho(0, -1)] + 1 \} + \varrho(1, 0) \mathfrak{W}(0, 0) [\varrho(0, 1) + \varrho(0, -1)] | M \rho_s \rangle\rangle \quad (60)$$

Using the same procedure as that used previously for the calculation of Eq. (59), this matrix element yields,

$$R_{ba} = -\beta^2 R_{cb} \left\{ \frac{G_{ab}(1, 0)}{G_{ac}^{-1}(1, 1) - \frac{\beta^2}{G_{bc}^{-1}(1, 2) - \frac{\beta^2}{\ddots}}} + (G_b^a + G_c^b - G_c^a) [G_{ab}(0, 1) + G_{ba}(0, -1)] \right\} \times \frac{1}{1 - \beta^2 G_b^a + G_a^b G_{ab}(0, 1) + G_{ba}(0, -1)}, \quad (61)$$

where

$$G_i^f = G_{i;i;i}(0, 0) - G_{i;i;f}(0, 0).$$

It can be seen here that, due to the near-resonance conditions, the interference terms R_{ba} affect the two-photon resonance at $\omega_1 + \omega_2$, but not that at $\omega_1 - \omega_2$. This is because the matrix elements of $\mathfrak{W}(1, -1) \varrho(0, -1)$ vanish since $\varrho(0, -1)$ is diagonal in $|ba^+\rangle$ and the $G(1, -1)$ in $\mathfrak{W}(1, -1)$ is diagonal in $|ac^+\rangle$; but M does not transfer $|ba^+\rangle$ to $|ac^+\rangle$ as can be seen from the list in Eq. (56).

The interference term R_{ba} has often been either omitted, Refs. 4, 6, and 7, in the usual perturbation treatment of multiphoton processes or neglected,¹⁸ by assuming that their saturative effect is small when the level separation ω_{ab} is small. It can be seen from Eq. (56) that whenever

$$\frac{\sinh(\omega_{ab}/2kT)}{\sinh(\omega_{bc}/2kt)} \ll e^{\omega_{ab}/kT},$$

the interference term can effectively be neglected and R_{cb} is the predominant effect of the strong perturbing field on the spectrum. To understand more clearly the physical significance of neglecting the saturative effects one can compare R_{ba} of Eq. (61) with Eq. (80) of I which represents the two-level saturation effect. The last factor in Eq. (61) is identical with the correction factor in (I.80) for the levels a, b . This term is then coupled by the terms in the first bracket of Eq. (61) to the multiphoton processes contained in R_{cb} .

Finally, it can be seen that when ω_{ab}/kT is not negligible with respect to ω_{bc}/kT , the interference terms can play an important role. This has been pointed out previously by Hansch and Toscher⁵ in their treatment of a three-level gas laser. Their result is equivalent to ours if only $G_{bc}(0, 1)$ and $G_{ac}(1, 1)$ are included as the near-resonance terms in Eq. (56) and all other terms neglected. This approximation is valid when $\omega_1 \approx \omega_{bc}$ and $\omega_2 \approx \omega_{ab}$.

A physical insight into the various effects contained in R_{cb} can be obtained by taking the imagi-

nary part of χ (proportional to the spectral power absorbed), neglecting the interference terms (R_{ba}) and all but the two-photons terms.

Using the impact-approximation Green's functions of Eq. (46), we obtain,

$$\text{Im} R_{cb} = R_{cb}'' = \left(\gamma_{bc} + \frac{\beta^2 \gamma_{ac}}{\Omega^+} + \frac{\beta^2 \gamma_{ac}}{\Omega^-} \right) B^{-1}, \quad (62)$$

where

$$B = \left(\Delta \omega_{bc} - \beta^2 \frac{\Delta \omega_{ac} + \omega_2}{\Omega^+} - \beta^2 \frac{\Delta \omega_{ac} - \omega_2}{\Omega^-} \right)^2 + \left(\gamma_{bc} + \beta^2 \frac{\gamma_{ac}}{\Omega^+} + \beta^2 \frac{\gamma_{ac}}{\Omega^-} \right)^2, \quad (63a)$$

$$\Omega^\pm = (\Delta \omega_{ac} \pm \omega_2)^2 + \gamma_{ac}^2, \quad (63b)$$

$$\Delta \omega_{if} = \omega_1 - \omega_{if}, \quad (63c)$$

when ω_1 is used to probe the $b \rightarrow c$ transition and ω_2 is not resonant with ω_{ab} the most important contribution to the spectra is contained in the first term in Eq. (62) and can be written as,

$$R_{cb}''(\omega_1 \approx \omega_{bc}) \approx \frac{\gamma_{bc}}{B} = \frac{\gamma_{bc}}{(\Delta \omega_{bc} + \Delta)^2 + (\gamma_{bc} + \Gamma)^2}, \quad (64)$$

where

$$\Delta = \beta^2 \frac{2\omega_{ab}}{\omega_{ab}^2 - \omega_2^2}$$

and

$$\Gamma = \beta^2 \frac{\gamma_{ac}(\omega_{ab}^2 + \omega_2^2)}{(\omega_{ab}^2 - \omega_2^2)^2}.$$

This is a Lorentz shaped resonance line at ω_{bc} , shifted and broadened by the dynamic Stark effect.¹⁹ When the perturbing field ω_2 is resonant with ω_{ab} , the shift becomes large, but also other terms in Eq. (62) become important and the spectrum is no longer composed of a single Lorentz shaped line.

When ω_1 is used to probe the $\omega_{ac} \pm \omega_2$ region of

the spectra, the resonant part of the first term in Eq. (62) now becomes

$$R''_{cb}(\omega_1 \approx \omega_{ac} \pm \omega_2) \approx \frac{\beta^2}{(\omega_{ab} \mp \omega_2)^2} \frac{\gamma_{ac}}{\Omega^{\pm}}. \quad (65)$$

This represents two Lorentzian lines centered at $\omega_1 = \omega_{ac} \pm \omega_2$. These are the two-photon transition lines or "satellite lines," observed when $\beta^2/(\omega_{ab} \mp \omega_2)^2$ is large enough so that the resonance line at ω_{bc} does not drown them. Equation (65) is the usual strong-field perturbation theory result for the two-photon transition.⁶ As the strong-field parameter β is increased, the other terms in R''_{cb} become important. Ordinary perturbation theory breaks down and the spectrum can no longer be described as a series of Lorentzian lines. In addition, as the strong field approaches resonance with the $a-b$ transition ($\omega_2 \approx \omega_{ab}$), the Stark shifts of the resonance line at ω_{bc} and the asymmetry of the multiphoton transitions become pronounced. These effects are illustrated in the calculations in Sec. V.

V. CALCULATIONS

Numerical calculations of the continued fractions, Eqs. (59) and (61), have been performed in order to display the effects discussed qualitatively in the previous sections. Since the dynamic Stark shifts and multiphoton effects are contained in Eq. (59), we choose a case in which this is the only important contribution, i.e., a case for which $\omega_{ab} \ll \omega_{bc}$. The case chosen corresponds roughly to the Stark-broadened $4D-2P$ permitted and $4F-2P$ forbidden transition in He which has been extensively studied for use in plasma diagnostics.^{9,20-22} More detailed calculations of this effect, taking into account space degeneracy and the correct Stark-effect eigenstates (which lifts the restriction on the forbidden transition) will be studied in a separate publication. This case is of particular interest in that it enables a detailed study of nonequilibrium stationary plasmas.²³

In Fig. 4(a), the spectrum for the case $\omega_2 < \omega_{ab}$ is presented with various values of β^2 . The range in β^2 from 0.01 to 10 cm^{-2} corresponds for He to roughly 0.25–8 kV of rms power in the perturbing-field strength. For convenience γ_{bc} has been taken equal to γ_{ac} . For this particular value of ω_2 , the resonance line (along with the even numbered satellites which appear symmetrically about it) shifts toward lower frequencies, while the odd-numbered satellites (symmetrically spaced about the position of the forbidden transition) shift toward higher frequencies. The opposite is true when $\omega_2 > \omega_{ab}$. In addition, as β^2 is increased, increasing numbers of satellites are seen to ap-

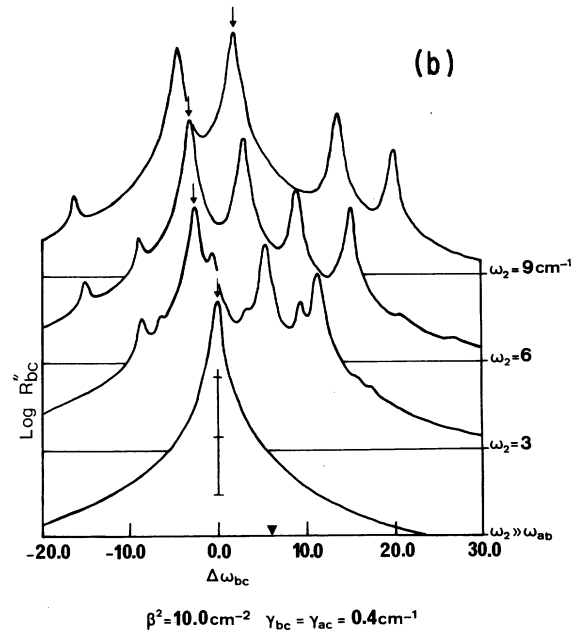
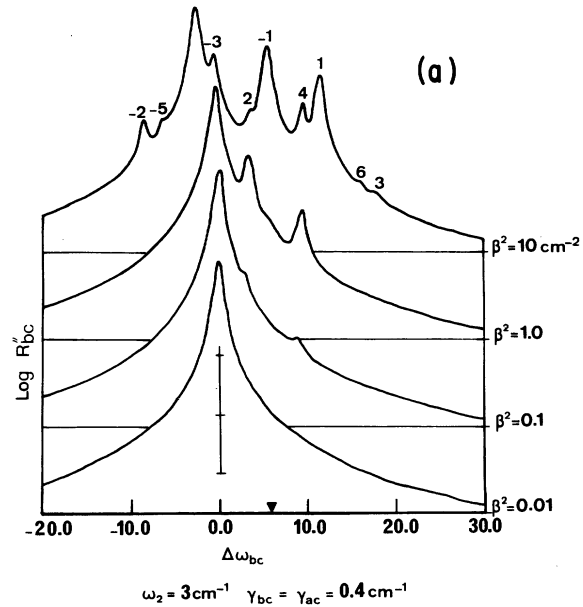


FIG. 4. Contribution of the imaginary part of Eq. (59) to the linear response of a three-level system to a monochromatic field of frequency ω_1 in the presence of a saturating field of frequency ω_2 . The horizontal axis measures the frequency difference (in cm^{-1}) from the unperturbed position of the resonance transition ω_{bc} . The arrow indicates the frequency $\omega_{ab} = 6 \text{ cm}^{-1}$. (a) Case $\omega_2 < \omega_{ab}$ is presented for different values of the strong-field parameter β^2 with linewidth parameters $\gamma_{bc} = \gamma_{ac}$. (b) Case $\beta^2 = 10 \text{ cm}^{-2}$ is presented for various values of the saturating-field frequency with fixed linewidth parameters, $\gamma_{bc} = \gamma_{ac}$. The arrow indicates the resonance line.

pear, some of them becoming almost as important as the resonance line. The radiation broadening of the resonance line with increasing perturbing-field strength can also be seen in this figure. In Fig. 4(b) the variation of the direction of the dynamic Stark shift, as a function of the perturbing-field frequency for a given field strength, is displayed. The lower curve is the resonance line itself (obtained when the perturbing field is either absent or of very high frequency). As the frequency increases, the resonance line marked by an arrow in this figure and associated even-numbered satellites shift to lower frequency while the odd-numbered satellites shift to higher frequency [as noted previously in Fig. 4(a)] until $\omega_2 = \omega_{ab}$. For $\omega_2 > \omega_{ab}$ the shift is reversed until $\omega_2 \gg \omega_{ab}$ when the satellites disappear and the resonance line returns to its original position. The curve for $\omega_2 = 6 \text{ cm}^{-1}$, which is $\omega_2 = \omega_{ab}$, displays the phenomenon known as the splitting of the resonance line. Here, the satellite at $\omega_1 = \omega_{bc} - \omega_2$ [the satellite labeled -1 in Fig. 4(a)] is almost as important as the resonance line itself and the minimum between this satellite and the resonance line occurs at the unperturbed position of the resonance line.

The convergence of the continued fraction, Eq. (59) is shown in Fig. 5. Here the spectrum is displayed for calculations involving N terms in the continued fraction. The positions and shapes of the spectral resonances become stable after taking only 12 terms in the continued fraction for

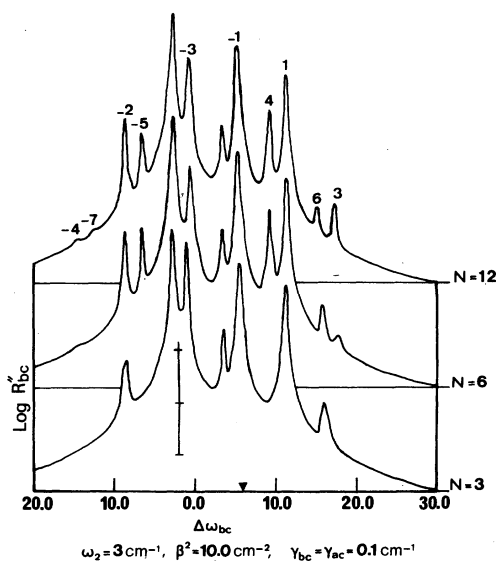


FIG. 5. Effect of including N terms in the imaginary part of Eq. (59) for fixed values of the strong-field parameter and frequency. Curves for $N > 12$ are not presented since they are identical to the curve $N = 12$ for these values of β^2 and ω_2 .

this case. This is in accord with the approximate rule of stability, $\beta^2/N\omega_2^2 < 1$, obtained from an analysis of Padé approximants.²⁴ Thus, the smaller the perturbing frequency, or the stronger its field strength, the more terms must be taken to calculate correctly the spectrum. Finally, in Fig. 6, the effect of changing the ratio of the width of the forbidden transition to that of the permitted line is shown. The lower curve corresponds to a resonance line ten times broader than the forbidden line. The upper curve shows the reverse situation. Thus, in the lower curve, the satellites ± 2 (about the permitted transition) are drowned by the resonance line, but those about the forbidden line (governed by its linewidth parameters) are distinctly visible. The upper curve shows the appearance of the drowned ± 2 satellites and the smearing out of the formerly sharp ± 1 satellites. This demonstrates the dangers involved in attempting to use satellites for a diagnosis of the field in a plasma if the linewidth parameters are not known. Conversely in situations in which the fields used are of known strength and frequency, Fig. 6 shows clearly the possibility of using this effect to obtain the line-shape parameters.

VI. VELOCITY EFFECTS

If the motion of the molecules in the absorbing system is taken into account, the resonance frequency becomes a function of the molecular velocity through the Doppler effect. Thus, the Liouvilian of the unperturbed molecule, i.e., that part projected out of the Green's function in Eq. (24a), now contains a translational term.¹⁵ In addition,

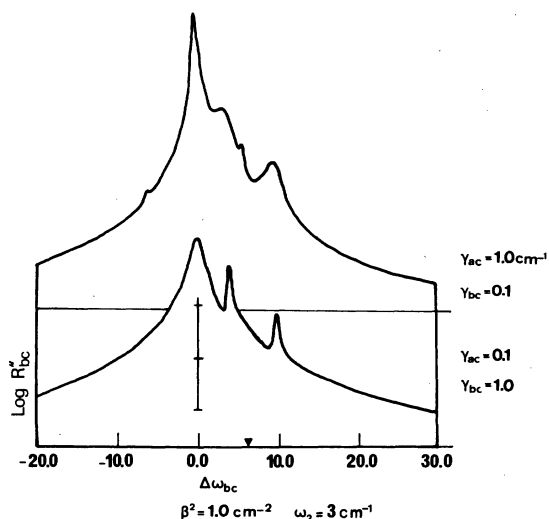


FIG. 6. Effect of changing the linewidth parameters on the spectra described by the imaginary part of Eq. (59).

velocity effects may enter through the dependence on velocity of the tetradic self-energy $\Sigma_c(\omega)$.^{15,16}

Treating the various velocity states as vectors (in Liouville space), $\Sigma_c(\omega)$ is a matrix defined on this space. We shall discuss here only the case where $\Sigma_c(\omega)$ is completely degenerate in velocity space. The Doppler shift is introduced when μ is replaced by $\mu e^{-i\vec{k}\cdot\vec{r}}$ as in Eq. (1). In the classical-path approximation, the molecular translation term simply adds $\vec{v}\cdot\vec{k}$ to the Liouvillian where \vec{v} is the molecular velocity. Thus, the linear-response Green's functions appearing in the previous sections are replaced by

$$G(n, m) = [n\omega_1 + m\omega_2 - L_0 - \Sigma_c(n\omega_1 + m\omega_2) + n\vec{k}_1 \cdot \vec{v} + m\vec{k}_2 \cdot \vec{v}]^{-1} \quad (66)$$

and the susceptibility corresponding to Eq. (37) becomes

$$\begin{aligned} \chi(k_1, \omega_1) E_1 &= -(N/V) \sum_{\pm} \sum_{i=1,2} \text{Tr} \langle \langle 1_1, 0_2 | \mu e^{-i\vec{k}\cdot\vec{r}} \\ &\quad \times D\mathcal{S}DM e^{+i\vec{k}_i\cdot\vec{r}} \mathcal{G}_i^{\pm} \rho_s | 0_1, 0_2 \rangle \rangle, \quad (67) \end{aligned}$$

where \mathcal{G} is now defined in terms of the G of Eq. (66). In Eq. (67), the single-molecule Liouville subspace now includes the translational momentum states of the absorbing molecule in addition to the internal states included previously. The density matrix ρ_s contains the momentum distribution function of the molecules and the trace operation includes a trace over these momentum states. If the tetradic self-energy is independent of the velocity a Voigt profile is obtained instead of the Lorentz profile in the linear response and impact approximations. For the nonlinear response, complicated momentum integrals are obtained, which have been evaluated approximately in third-order perturbation theory by Hansch and Toschek.⁵ Various effects such as directional anisotropy of the spectral line shape⁵ and line-narrowing effects in coupled Doppler-broadened transitions²⁵ can be studied using the velocity-dependent formalism.

The dependence of Eq. (67) on the momenta needs some further comment. In a homogeneous (translationally invariant) gas sample, the averaging process required that the sum of all k -dependent exponents vanish. Here this is automatically observed since in Eq. (67) each $e^{i\vec{k}\cdot\vec{r}}$ is canceled by a corresponding $e^{-i\vec{k}\cdot\vec{r}}$ in each diagram. However, the various linear-response functions, $G(\Omega)$ (treated as diagonal operators in HNR), are generally momentum dependent and should rather be written as $G(K, \Omega)$ where, corresponding to the harmonics-number combination $\Omega = \sum_a n_a \omega_a$, we

have $\vec{K} = \sum_a n_a \vec{k}_a$ with \vec{k}_a the wave vector of the mode with angular frequency ω_a .

VII. CONCLUSION

The theory developed above presents a treatment of various nonlinear radiation processes using as a basis the methods of linear-response theory which have been extensively used in spectroscopic line-shape problems. This, combined with techniques of quantum-field theory for the summation to all powers of the applied field (treated classically) permits a simple and unified presentation of phenomena usually studied separately. In addition, line-broadening phenomena are introduced in a clear and uncomplicated manner so that the spectroscopic problems treated can yield the atomic parameters unambiguously.

The application of the theory to the problem of a three-level molecular system interacting with a weak-probe field and a strong perturbing field gives results in agreement with previous work, within the range of validity. For example, the nonlinear response yields a classical counterpart of the quantum-mechanical dressed-atom propagator. The nonlinear interference terms obtained by including stimulated emission processes, correspond to those introduced in previous work.⁵ Also, dynamic Stark shifts and multiphoton "satellites" have been derived to all orders.

Special emphasis has been put on the various line broadening mechanisms contributing to the spectral shape. Thus, cross-relaxation effects, inelastic collisions, and velocity effects can be included in the formalism. In addition, it has been pointed out how information on the atomic parameters of forbidden lines may be obtained.

The above formulation of nonlinear relaxation processes in terms of linear-response functions permits a clearer understanding of the physical processes involved. In this manner, it has been shown that the detailed calculation of the optical spectra of systems in strong-radiation fields can be performed with rigor comparable to that used in the usual weak-field spectroscopy.

In fact, in addition to the work of Autler and Townes,⁴ cited previously, rigorous solutions of the Liouville equation have been recently used with success^{26,27} in the domain of rf spectroscopy combined with optical pumping.²⁸ The perturbative solutions of the Cohen-Tannoudji group referred to above have been obtained as approximations to continued-fraction solutions similar to those which occur in this article. This, again, is evidence of the fact that the nonlinear terms correspond classically to the "dressing" of the atom. The relationship between these continued-fraction

solutions and the present work follows from the fact that in both cases one calculates the response of the system by computing matrix elements of the density operator. In the rf case, however, since the pumping field is monitored, it is possible to reduce the calculation to the two-level, one strong-field problem which was discussed in I, Sec. VIII, in the resonant approximation. If the nonresonant terms neglected in I are included so that Fig. 2 of I contains terms $G(2)$, $G(3)$, etc., then the renormalization techniques described in this article can be used. This results in the replacement of $G_{ab}(\pm 1)$ by $\mathcal{G}_{ab}(\pm 1)$ [where $\mathcal{G}_{ab}(\pm 1)$ is the solution of a Dyson equation corresponding to the one written here in Eq. (55)]. This result is then the same (with appropriate changes in the meaning of the various parameters) as that presented, for example, in Ref. 27 for the case of longitudinal pumping, where multiphoton transitions are also observed. The case of transverse pumping in which resonances due to virtual transitions are observed^{29,30} is particular to experiments involving level crossing. However, the problem is formally the same, yielding again continued-fraction solutions^{31,32} and can also be treated by the methods described here.

The present work suggests several subjects which will be considered in a future publication. The problem of including velocity effects is of great current interest. Using tunable-laser spectroscopy it is now possible to study the velocity dependence of the tetradic self-energy.³³ Including these effects in the manner described in Sec. VI will result in information on the interference of velocity and collisional line-broadening effects which have a direct bearing on the output power of lasers as a function of frequency.³⁴ This problem is closely related to the Dicke narrowing

effect which has been extensively studied in theoretical weak-field spectroscopy.³⁵

It is intended to recalculate the example presented in Sec. V using nonparity eigenfunctions. This will enable a better comparison with the experiments performed on partially ionized He which have displayed anomalous "satellites" not explained by the usual parity-eigenstate theory.²³ Nonparity eigenstates occur since in problems involving charged-particle broadening the atom is subject to a quasistatic electric field owing to the plasma ions and one should use the Stark-effect atomic wave functions which are linear combinations of parity eigenfunctions.

The interference terms R_{ba} should be studied with a view toward understanding their importance in situations where the level spacing is such that they may play a role. In this respect it is to be noted, that even when the levels involved are completely saturated by the strong field, these terms are not zero.

Finally, the expression obtained for the susceptibility in terms of a continued fraction may be related to the Mori hierarchy,³⁶ to which it bears a formal resemblance. It would be interesting to study this idea in the context of a more general form of nonlinear-response theory.

ACKNOWLEDGMENTS

One of the authors (L.K.) would like to thank Professor R. Coulon and Professor M. Sirugue-Colin for their hospitality during his stay at the Laboratoire des Interactions Moleculaires and the U. E. R. de Physique, Université de Provence. In addition, A. Ben-Reuven would like to express his appreciation to Professor I. Oppenheim for his hospitality at the Department of Chemistry, M.I.T.

*Work supported in part by the National Science Foundation.

†Permanent address: Department of Physics, Howard University, Washington, D. C. 20001.

‡Permanent address: Department of Chemistry, Tel Aviv University, Tel Aviv, Israel.

¹A. Ben-Reuven and L. Klein, *Phys. Rev. A* **4**, 753 (1971).

²W. E. Lamb, Jr., *Phys. Rev.* **134**, A429 (1964).

³A. Javan, *Phys. Rev.* **107**, 1579 (1957).

⁴S. Autler and C. Townes, *Phys. Rev.* **100**, 703 (1955).

⁵T. Hansch and P. Toschek, *Z. Phys.* **236**, 213 (1970).

⁶W. Hicks, R. Hess, and X. Cooper, *Phys. Rev. A* **5**, 490 (1972).

⁷M. Baranger and B. Mozer, *Phys. Rev.* **123**, 25 (1961).

⁸R. Karplus and J. Schwinger, *Phys. Rev.* **73**, 1020 (1948).

⁹A. Di Giacomo, *Nuovo Cimento* **14**, 1082 (1959).

¹⁰A. Ben-Reuven, *Phys. Rev. Lett.* **14**, 349 (1965); *Phys. Rev.* **145**, 2 (1966).

¹¹M. Baranger, *Phys. Rev.* **111**, 481 (1958); **111**, 494 (1958); **112**, 855 (1958).

¹²R. Kubo, in *Lectures in Theoretical Physics*, edited by W. Brittin and R. Dunham (Interscience, New York, 1959), Vol. I, p. 120.

¹³R. Zwanzig, in *Lectures in Theoretical Physics*, edited by W. Brittin, B. Downs and J. Downs (Interscience, New York, 1961), Vol. 3, p. 106.

¹⁴U. Fano, *Phys. Rev.* **131**, 259 (1963).

¹⁵A. Ben-Reuven, *Phys. Rev.* **4**, 215 (1971).

¹⁶A. Ben-Reuven, *Adv. Chem. Phys.* (to be published).

¹⁷A. Ben-Reuven, *Phys. Rev.* **141**, 34 (1966).

¹⁸C. Cohen-Tannoudji and S. Haroche, *J. Phys.* **30**, 125 (1969); **30**, 153 (1969).

- ¹⁹M. Mizushima, *Phys. Rev.* 133, 414 (1964).
²⁰W. Cooper and H. Ringler, *Phys. Rev.* 179, 226 (1969).
²¹H. Kunz and H. Griem, *Phys. Rev. Lett.* 21, 1048 (1968).
²²H. Griem (unpublished); D. D. Ringler, *J. Phys. B* 4, L7 (1971).
²³H. Ringler, *Phys. Lett. A* 41, 15 (1972).
²⁴M. Cadilhac (private communication).
²⁵M. Feld and A. Javan, *Phys. Rev.* 177, 540 (1969); B. Feldman and M. Feld, *Phys. Rev. A* 5, 899 (1972).
²⁶S. Swain, *J. Phys. A* 6, L169 (1973); 6, 192 (1973); 6, 1919 (1973).
²⁷S. Stenholm, *J. Phys. B* 5, 878 (1972); 5, 890 (1972); 6, L240 (1973).
²⁸W. Happer, *Rev. Mod. Phys.* 44, 169 (1972); C. Cohen-Tannoudji, in *Cargese Lectures in Physics 1968*, edited by M. Levy (Gordon and Breach, New York, 1969), p. 347.
²⁹S. Haroche, *Ann. Phys. (Paris)* 6, 189 (1971); 6, 327 (1971).
³⁰C. Cohen-Tannoudji, J. Dupont-Roc, and C. Fabre, *J. Phys. B* 6, L218 (1973).
³¹S. Stenholm and C. Aminoff, *J. Phys. B* 6, 2390 (1973).
³²N. Tsukada and T. Ogawa, *J. Phys. B* 6, 1643 (1973).
³³W. Demtroder, *Phys. Rep.* 7, 225 (1973).
³⁴P. Berman and W. Lamb, Jr., *Phys. Rev.* 187, 221 (1969); *Phys. Rev. A* 2, 2435 (1970); 4, 319 (1970).
³⁵R. H. Dicke, *Phys. Rev.* 89, 472 (1953); J. P. Wittke and R. H. Dicke, *Phys. Rev.* 103, 620 (1956); L. Galatry, *Phys. Rev.* 122, 1218 (1961); E. Smith, J. Cooper, W. Chappell, and T. Dill, *J. Quant. Spectrosc. Radiat. Transfer* 11, 1547 (1971).
³⁶H. Mori, *Prog. Theor. Phys.* 33, 423 (1965); 34, 399 (1965).